Generalized additive modelling of daily precipitation extremes and their climatic drivers

Mari R. Jones
Stephen Blenkinsop
Hayley J. Fowler
David B. Stephenson
Christopher G. Kilsby

NCAR/TN-501+STR

May, 2013

NCAR Technical Notes

National Center for Atmospheric Research
P. O. Box 3000
Boulder, Colorado
80307-3000
www.ucar.edu

NCAR TECHNICAL NOTES

http://library.ucar.edu/research/publish-technote

The Technical Notes series provides an outlet for a variety of NCAR Manuscripts that contribute in specialized ways to the body of scientific knowledge but that are not yet at a point of a formal journal, monograph or book publication. Reports in this series are issued by the NCAR scientific divisions, serviced by OpenSky and operated through the NCAR Library. Designation symbols for the series include:

EDD – Engineering, Design, or Development Reports
Equipment descriptions, test results, instrumentation, and operating and maintenance manuals.

IA – Instructional Aids
Instruction manuals, bibliographies, film supplements, and other research or instructional aids.

PPR – Program Progress Reports
Field program reports, interim and working reports, survey reports, and plans for experiments.

PROC – Proceedings
Documentation or symposia, colloquia, conferences, workshops, and lectures. (Distribution maybe limited to attendees).

STR – Scientific and Technical Reports
Data compilations, theoretical and numerical investigations, and experimental results.

The National Center for Atmospheric Research (NCAR) is operated by the nonprofit University Corporation for Atmospheric Research (UCAR) under the sponsorship of the National Science Foundation. Any opinions, findings, conclusions, or recommendations expressed in this publication are those of the author(s) and do not necessarily reflect the views of the National Science Foundation.

National Center for Atmospheric Research
P. O. Box 3000
Boulder, Colorado 80307-3000

NCAR/TN-501+STR
NCAR TECHNICAL NOTE

2013-05

Generalized additive modelling of daily precipitation extremes and their climatic drivers

Mari R. Jones
NCAR Earth System Laboratory, Boulder CO, USA
Stephen Blenkinsop
School of Civil Engineering and Geosciences, Newcastle University, Newcastle-upon-Tyne, UK
Hayley J. Fowler
School of Civil Engineering and Geosciences, Newcastle University, Newcastle-upon-Tyne, UK
David B. Stephenson
Exeter Climate Systems, Mathematics Research Institute, University of Exeter, Exeter, UK
Christopher G. Kilsby
School of Civil Engineering and Geosciences, Newcastle University, Newcastle-upon-Tyne, UK

NCAR Earth System Laboratory
Mesoscale and Microscale Meteorology Division

NATIONAL CENTER FOR ATMOSPHERIC RESEARCH
P. O. Box 3000
BOULDER, COLORADO 80307-3000
ISSN Print Edition 2153-2397
ISSN Electronic Edition 2153-2400

Table of Contents

1 List of Tables

2 List of Figures

3 Acknowledgments

NCAR is funded by the National Science Foundation. This work was part of a NERC funded Postgraduate Research Studentship NE/G523498/1 (2008-2012; MJ) and was supported by a NERC post-doctoral Fellowship award NE/D009588/1 (2006-2010; HJF). The R analysis software (R Core Development Team, 2011) and packages VGAM (Yee, 2011) and extRemes (Gilleland *et al.*, 2009) were used for all analysis in this paper. Thanks are also due to Dr Renato Vitolo for his assistance with programming and analysis, and to Dr Rick Katz for comments on an earlier version of this document which have greatly improved the clarity.

4 Introduction

Detection of changes in climate responses is essential to facilitate appropriate adaptation action to be taken by decision makers; however, detection of changes in the extremes may not be possible in the desired timescale for action (Fowler *et al.*, 2010). It is hoped that by understanding current mechanisms driving extreme precipitation and the risks, or likely impacts, that the uncertainty surrounding future projections can be reduced (Tebaldi *et al.*, 2006), providing a realistic decision framework for designers and planners. A recent focus on trend analyses within a changing climate has revived interest in distinguishing climatic variability from "real" changes (Koutsoyiannis, 2003; Sakalauskiene, 2003; Ammann *et al.*, 2007). Cohn and Lins (2005) observed that long term persistence is often suggestive of a trend, as fractional noises arising from climatic variability often display multiple 'features' including trends and cycles. Long established hydrological practice assumes that, for the purposes of design, observational series are stationary (Matalas, 1997; Lins and Cohn, 2011); however, this may no longer be appropriate for extreme hydrology if

stationarity cannot be assumed over the engineering design life (Milly *et al.*, 2008), suggesting that more sophisticated analysis tools are required.

The variability of extreme precipitation event frequency from year to year can be assessed through the dispersion of the annual count of events exceeding a high threshold. Persistence is particularly evidenced by 'clusters' of years (referred to as *overdispersion*) with high and low frequencies of floods or heavy precipitation (Villarini *et al.*, 2009). The natural sequence of these extreme events will display some irregularity, which may appear within a reasonably short series to be overdispersion but following removal of external influence, such as seasonality, will be homogeneously Poisson distributed (Serinaldi and Kilsby, 2013). However, it is the occurrence of several periods of heavy precipitation in quick succession which may generate flood conditions. Many have examined trends in the return frequency of extreme events (Fowler and Kilsby, 2003a; Moberg and Jones, 2005; Fowler *et al.*, 2010; Jones *et al.*, 2012) or the number of wet days per year (Pryor *et al.*, 2009; Li *et al.*, 2011), and some studies have examined changes to the timing and frequency of peak-over-threshold events (e.g. Fowler and Kilsby, 2003b), but only a few have acknowledged the importance of several events occurring in succession or specifically assessed whether the intra-year dispersion is changing (e.g. Villarini *et al.*, 2012).

There is strong evidence that independent extreme precipitation events are not dispersed regularly in time, rather they follow a seasonal non-homogeneous Poisson distribution (Tramblay *et al.*, 2011); however, the temporal relationship between these independent events is often ignored. Many extreme value analyses focus on the magnitude of the events above a certain threshold and their annual return frequency (Davison and Smith, 1990; Fawcett and Walshaw, 2007), rather than the interval between these events. Others examine the longevity of a spell of successive excesses (Furrer *et al.*, 2010), identifying independent events by a minimum number of days below the threshold. Yet the dispersion of extreme events within a particular year or season is also of interest for flood risk managers. Extreme precipitation responses to seasonality and long-term patterns in atmospheric drivers present a highly complex relationship which cannot be examined with standard statistical tools. Improved estimates of event frequency and magnitude could be achieved using extreme value parameters estimated from linear models of covariate terms, e.g. seasonality (Tramblay *et al.*, 2011). Linear models, of varying degrees of complexity, facilitate improved estimates of the covariate dependent parameter estimates and can be used to describe any long-term changes in behaviour (Furrer and Katz, 2008).

Generalized Linear Models (GLM) are effective in modelling daily precipitation event occurrence and their dependence on atmospheric circulation patterns (Sapiano *et al.*, 2006), and have been applied to many complex time series (e.g. Furrer and Katz, 2008; Maraun *et al.*, 2011), although they can over-simplify data or processes which are highly random from year to year, such as intra-year variability (Allamano *et al.*, 2011), or precipitation responses to long term atmospheric oscillations (Chavez-Demoulin and Davison, 2005). An enhancement to the GLM is that of Generalized Additive Models (GAM; Hastie and Tibshirani, 1990) based on smoothly varying flexible predictors. The GAM has been widely adopted as an effective model for strongly seasonal or forced responses (Wood, 2006; Villarini and Serinaldi, 2011), as well as for multi-annual atmospheric responses (Morton and Henderson, 2008; Underwood, 2009; Mestre and Hallegatte, 2009), and is considered particularly appropriate for use here. GAMs have gained popularity in assessing data with a strong time-varying component and atmospheric dependence (Hyndman and Grunwald, 2000), as well as for identifying whether long-term behavioural changes are occurring (Underwood, 2009). GAMs have been widely employed in other disciplines to model the health impacts of air pollution or long term variability in biota spatial density, but rarely applied in hydrology (Morton and Henderson, 2008; Underwood, 2009).

The direct application of GLMs or GAMs in extreme value distributions is computationally difficult, as the distributions are limited to the exponential family, premised on the mean of the distribution. A more readily applied method is that of Vector Generalized Additive Models (VGAM), introduced by Yee and Wild (1996), which allows a broader class of statistical models to be derived from the data, and extend the family of applicable distributions beyond the exponential.

The aim of this research was to develop a robust statistical tool with which to test changes in the frequency and magnitude of extreme daily precipitation over a spatially coherent region, rather than for individual locations. The objective was to characterise the inter-annual variability of extreme event frequency, which generate a seasonally over-dispersed Poisson distribution, and the associated magnitude of these events. The modelling technique is one which could be applied in many regions of the world, but was specifically focussed on an application to UK extreme daily precipitation.

Eventual application of the VGAMs to very heavy daily precipitation totals across the UK will facilitate robust assessments of: (i) variability in the arrival rate of heavy precipitation throughout the year; (ii) whether long term trends exist in the frequency

distribution; and, (iii) apparent changes in the seasonal distribution. In contrast with other spatial analyses of extreme precipitation, a point process is applied to pooled block maxima and spatially pooled POT event frequency to simulate the event intensity and intra-annual rate of occurrence, respectively (e.g. Katz *et al.*, 2002; Eastoe and Tawn, 2010). This contrasts with other regional frequency analyses which make use of the regionally pooled block maxima (e.g. Hosking and Wallis, 1997; Jones *et al.*, 2012) or POT maxima (e.g. Madsen *et al.*, 1997) to estimate event magnitudes and the annual probability of occurrence. The research also differs from Maraun *et al.* (2011), who developed monthly models of daily precipitation maxima for individual sites dependent on proxies of atmospheric circulation patterns. Their sinusoidal Vector Generalized Linear Models (VGLM) over-simplified the observed seasonal responses and did not examine the inter-event arrival rate of extreme precipitation events.

The remainder of this article first summarises the data sets used in Section 2 and the statistical theory to be applied in Section 3. It then describes the selection of the VGAM parameters and the development of the statistical model for extreme daily precipitation arrival rate and magnitude in Section 4 before describing the model validation in Section 5. Discussion and conclusions are presented in Section 6.

5 Data

5.1 Daily UK Precipitation

While gridded data series provide a more reliable temporal series, with fewer missing data, the interpolated data may miss localised intense storms and underestimate point maxima. As this underestimation can be considerable for small radius convective storms, and the focus of the research was on extreme events, individual station observations were selected for this research. Daily precipitation observations from 199 observation stations across the UK were used, illustrated in Figure 1 in relation to the newly defined UK extreme rainfall regions (Jones *et al.*, 2013). Further details on the compilation of the data set, from records supplied on http://badc.nerc.ac.uk, and the homogeneity of the observations can be found in Jones *et al.* (2010, 2012). Annual Maxima were limited to the period 1961-2010 from each station series to develop the statistical models. Similarly, peak over threshold (POT) analyses, were identified from each station observation series over the period 1961-2010, using a station specific threshold for *very heavy wet days* (Q95; Alexander *et al.*, 2006), that is the 0.95 quantile of the wet day distribution. A wet day was defined as days receiving ≥1mm

precipitation, which has been shown to generate more reliable estimates of extreme value models by eliminating trace measures of precipitation (Moberg and Jones, 2005; Alexander *et al.*, 2006).

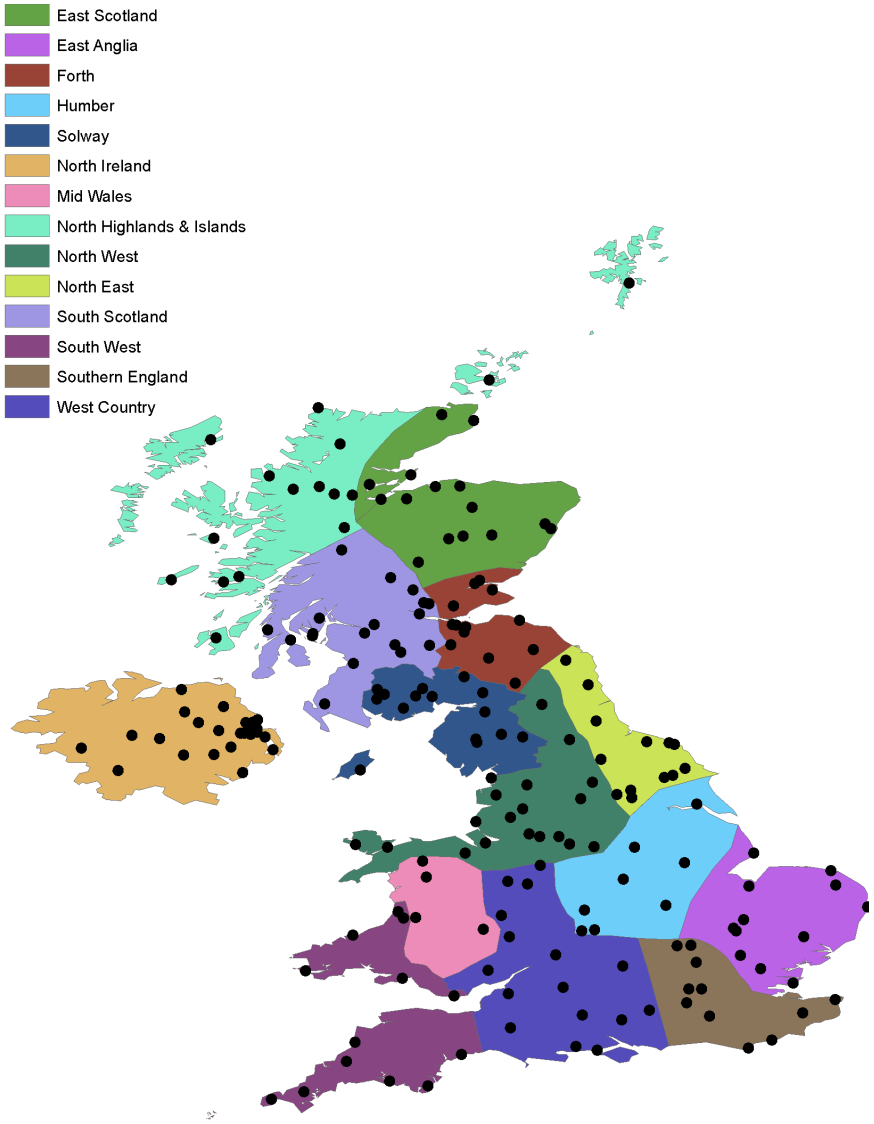

Figure 1 : Location of gauging stations in relation to the 14 extreme rainfall regions: North Highlands and Islands (NHI), East Scotland (ES), Forth (FOR), South Highlands (SH), North West (NW), North East (NE), North Ireland (NI), Solway (SOL), Humber (HU), South West (SW), Mid Wales (MW), West Country (WC), Southern England (SE), East Anglia (EA). Reproduced from Jones *et al.* (2013) Figure 5.

5.2 Temperature

As the moisture holding capacity of the atmosphere is governed by temperature, described by the Clausius-Clapeyron relationship for the moisture holding capacity of the atmosphere (e.g. Held and Soden, 2006), and recent warming trends are associated with enhanced water vapour (Gershunov and Douville, 2008; Coumou and Rahmstorf, 2012), appropriate covariates for daily extreme precipitation may be air temperature and sea surface temperature (SST), although others may also be important. Increases in North Atlantic SSTs

would enhance the hydrological cycle (Wang and Dong, 2010) due to increased evaporation over the ocean, leading to positive moisture anomalies in the hot air masses moving over the UK and Western Europe from the Atlantic. Extreme precipitation responses to SSTs have been demonstrated in several different regions (Karnauskas and Busalacchi, 2009; Muza *et al.*, 2009). Colman (1997) found a positive but weak correlation between the North Atlantic SST anomalies during January and February, and the England and Wales precipitation series. Lagged monthly North Atlantic SST is one of several strong predictors of summer flows in the River Thames (Wilby *et al.*, 2004); a positive correlation also exists between monthly North Atlantic SSTs and southwest England precipitation anomalies (Phillips and McGregor, 2002) and for summer rainfall in eastern England (Neal and Phillips, 2009). Data exploration using Poisson regression models, not shown, concluded that extreme precipitation frequency and intensity is significantly correlated with monthly SST for UK coastal waters.

Temperature does not vary as rapidly over the spatial domain as precipitation, so errors associated with gridded temperature observations are far less than those for gridded precipitation. Gridded observations provide a homogeneous series, with fewer missing values, and publicly available data sets have been fully quality controlled and documented, whereas individual station records may retain some errors or have longer periods missing. High-resolution gridded global data sets for monthly surface air temperature (1901-2005) for minimum, maximum and mean temperature (Mitchell and Jones, 2005) updated to 2009 (Jones and Harris, 2009) were obtained as 5° x 5° grid box averaged air temperatures.

The Met Office Hadley Centre compiled SST data set, HadSST2 (Rayner *et al.*, 2005), is a global gridded (5° x 5° boxes) data set of monthly averaged SST observations from 1850 to present constructed from the International Comprehensive Ocean-Atmosphere Data Set (ICOADS). All temperature and sea level pressure observations were obtained from the KNMI Climate Explorer (http://climexp.knmi.nl; Klein Tank *et al.*, 2002).

5.3 Sea Level Pressure

Connections between mean sea level pressure (MSLP) and temperature and precipitation patterns are also well established (e.g. Della-Marta *et al.*, 2007). The Met Office Hadley Centre's MSLP data set, HadSLP2r, is an update from 1850 to the present day of HadSLP2 (Allan and Ansell, 2006), constructed for a 5° x 5° global grid from monthly NCEP/NCAR reanalysis fields for 2005 onwards. The authors suggest that this series represents one of the best available for any historical investigation of the influences of large-scale atmospheric circulation patterns.

5.4 North Atlantic Oscillation Index

The North Atlantic Oscillation (NAO) index is a dipole of sea level pressures between Iceland and the southern tip of the Iberian Peninsula, measured either between Stykkishólmur and the Azores (Hurrell and Deser, 2009 and references therein) or Reykjavík and Gibraltar (Jones *et al.*, 1997). Positive (negative) phases represent enhanced (diminished) Icelandic Low and Iberian High pressure fields. The most profound effects of the NAO are displayed through winter time surface temperatures, storminess and precipitation across much of the Northern Hemisphere. In its positive phase, warm moist air from enhanced westerly flows move across Europe to generate dry conditions over southern Europe and North Africa, while reducing North Atlantic temperatures and creating wet conditions in northern Europe. Recent work has also correlated inter-decadal variability in storm patterns with fluctuations in large scale teleconnection patterns, finding positive NAO years to have a strong influence on UK storm intensity and frequency (Allan *et al.*, 2009).

Given that the centre of NAO action shifts over time, a principal component analysis of the NAO index (Hurrell, 1995), which is less sensitive to modal displacements (NOAA, 2011), is considered to be more reliable for the current application (Casty *et al.*, 2005; Allan and Ansell, 2006). Therefore, monthly time series derived from the leading EOF of monthly MSLP anomalies over the Atlantic sector (20-80N, 90W-40E) were obtained from the Climate Analysis Section, NCAR, Boulder.

6 Method

6.1 Extreme value distributions

The distribution of series maxima, such as the annual maximum of daily precipitation totals, can be approximated by the limiting Generalized Extreme Value distribution (GEV) where:

$$G(x;\mu;\sigma;\xi) = exp\left[-\left(1+\frac{\xi(x-\mu)}{\sigma}\right)^{-1/\xi}\right] \quad \text{where} \quad 1+\frac{\xi(x-\mu)}{\sigma} > 0 \qquad (1)$$

for the location $-\infty < \mu < \infty$, scale $\sigma > 0$ and shape $-\infty < \xi < \infty$ parameters.

The frequency of a series of daily observations exceeding a high threshold, u, with N events per year, follows an approximate Poisson distribution with arrival rate Λ. When u is sufficiently high and N is very small, the magnitude of the excesses over u approximately follows another form of extreme value distribution, the Generalized Pareto (GPD) with

parameters scale, $\tilde{\sigma} > 0$, and shape, $-\infty < \xi < \infty$. The GPD is directly linked to the GEV through the respective shape, ξ, parameters (Davison and Smith, 1990) as:

$$\begin{aligned} \xi_{GPD} &= \xi_{GEV} \\ \ln \Lambda &= -1/\xi \ln\left[1 + \frac{\xi(u-\mu)}{\sigma}\right] \\ \tilde{\sigma} &= \sigma + \xi(u-\mu) \end{aligned} \tag{2}$$

The combined extreme value and Poisson distribution is often referred to as an orthogonal Point Process (Katz *et al.*, 2002), where the notation arises from the property of orthogonality between Λ and the parameters $\tilde{\sigma}$ and ξ for all independent data (Chavez-Demoulin and Davison, 2005). For a more complete exposition on extreme value theory, refer to Coles (2001).

6.2 Linear and Additive Models

For a set of explanatory variables, $X_1,\ldots,X_n$, GLMs describe a response variable, Y, through an exponential family, such that the mean $E(Y_i) = \mu_i$ can be described by a smooth monotonic link function, $g(\mu_i)$, of the linear predictors, $\beta_i \mathbf{x_i}$ (Nelder and Wedderburn, 1972):

$$g(\mu_i) = \eta_i = \beta_0 + \beta_1 x_1 + \ldots + \beta_n x_n \tag{3}$$

Vector Generalized Linear Models (VGLM) extend the available model families beyond the exponential family to extreme value distributions, applying the $\eta_i(x)$ directly to each of the distribution parameters.

However, the complex relationship between the characteristic variables driving the non-homogeneous rate of event occurrence, such as inter-annual atmospheric fluctuations, demands a flexible statistical model which encompasses non-linear behaviour. The required flexibility can be incorporated by using a GAM (Hastie and Tibshirani, 1990) where the linear predictor term $g(\mu_i)$ becomes a summation of smooth non-linear functions f_y of the covariates of an exponential family:

$$g(\mu_i) = \eta \mathbf{x}_i = \beta_0 + f_1(x_1) + \ldots + f_n(x_n) \tag{4}$$

Model smoothness, f_j, is transformed into a linear model via linear basis functions, b, for each non-linear parameter of the explanatory variables $(\beta_1,\ldots,\beta_j)$, i.e.

$$f_j(x) = \sum_{j=1}^{q} b_j(x)\beta_j \tag{5}$$

The aim is to choose a basis dimension as close to f_j as possible so that data are neither over- or under-smoothed. As with GLMs, the family distribution can be expanded beyond the exponential using vector smoothers. The vector smoothers used in VGAMs fit a vector of smooth functions, f_j, to the vector measurements model with spline smoothers to minimise the quantity with a two term penalty on the lack of fit degree of smoothing (Yee, 2011). Hastie and Tibshirani (1990) recommend the use of a combination of several polynomials or p-splines to model the smooth function; this shifts the focus to a model driven representation, focussing on a model which is flexible without over- or under-smoothing the response. Smoothers are chosen by default, within the VGLM R computing package, which removes the subjectivity required to choose the degree of smoothness (Faraway, 2006; Yee, 2010).

Combined analyses of the frequency and magnitude of extreme events adopt either an orthogonal Poisson-GP approach, or a Point Process formulated from the GEV distribution using Equation 2. Strict criteria were employed to extract precipitation maxima, whereby a year was omitted if too many daily observations were missing (refer to Jones *et al.*, 2010 for details); while annual maxima were verifiable from other sources, POT were found to be less reliable. As a result, the spatially pooled data sets comprised many more annual maxima than POT maxima, making the GEV applied to block maxima a more suitable approach to estimate event magnitude. However, a key point of interest was the interval between extreme events, represented by a Poisson distribution. As a result, the relationship between the GEV, GP and Poisson distributions was manipulated, and a non-standard approach was adopted combining GEV and Poisson distributions to estimate magnitude and frequency. For ease of application and comparison of the eventual results, the VGAM was used for both the GEV and the Poisson distributions even though it is not strictly required for the latter, which is in the exponential family. The software's enhanced flexibility and functionality permits direct estimation of parameters, e.g. for the GEV and Poisson distributions which will be used later in the form:

$$
\begin{aligned}
\log \Lambda(x) &= \eta_1 = \beta_{0(1)} + f_{1(1)}\left(x_{1(1)}\right) + \ldots f_{n(1)}\left(x_{n(1)}\right) \\
\mu(x) &= \eta_2 = \beta_{0(2)} + f_{1(2)}\left(x_{1(2)}\right) + \ldots + f_{n(2)}\left(x_{n(2)}\right) \\
\log \sigma(x) &= \eta_3 = \beta_{0(3)} + f_{1(3)}\left(x_{1(3)}\right) + \ldots + f_{n(3)}\left(x_{n(3)}\right) \\
\log\left(\xi(x) + \frac{1}{2}\right) &= \eta_4 = \beta_{0(4)}
\end{aligned}
\tag{6}
$$

The shape parameter, ξ, is fit by default as an intercept only term as it is numerically difficult to estimate (Katz *et al.*, 2002; Yee and Stephenson, 2007).

7 Parameter Selection

7.1 Model Covariates

The arrival rate, Λ, of POT events follows an approximate non-homogeneous Poisson distribution, with a higher frequency during certain seasons which can give the impression of within-year clustering (Serinaldi and Kilsby, 2013); inter-annual fluctuations in event frequency are influenced by ocean-atmosphere coupling and climatic variability. These attributes suggest that the covariates which should be included in the model should encompass, as a minimum, seasonal and atmospheric components.

7.1.1 Seasonality

Seasonal variability in the intensity of UK daily precipitation extremes is well recognised, with the south tending to receive the highest daily accumulations during the summer, while in the northwest these occur later in the year (Fowler and Kilsby, 2003b). Examining the combined records of all UK stations, Rodda *et al.* (2009) observed that there is a distinct multimodal distribution in the occurrence of extremely wet days throughout the year, with peaks at mid-summer and late autumn. A smoothed 30-day running mean was applied to the relative frequency of Q95 events per day of the year for each of the 199 gauged records; refer to Figure 2 for two examples from the northwest and southeast of the UK. This approach removed anomalies arising from variability in the day of occurrence and differences in observation record length; sensitivity testing of the period used to calculate the running mean established that this multi-modality was not merely a spurious cyclical response arising from the calculation. The figures revealed considerable regional variation in the timing of extreme precipitation and the duration of the most "active" period for these events. This seasonal variation is an important factor in understanding within-year over-dispersion of extreme precipitation events, which in turn can generate flood conditions.

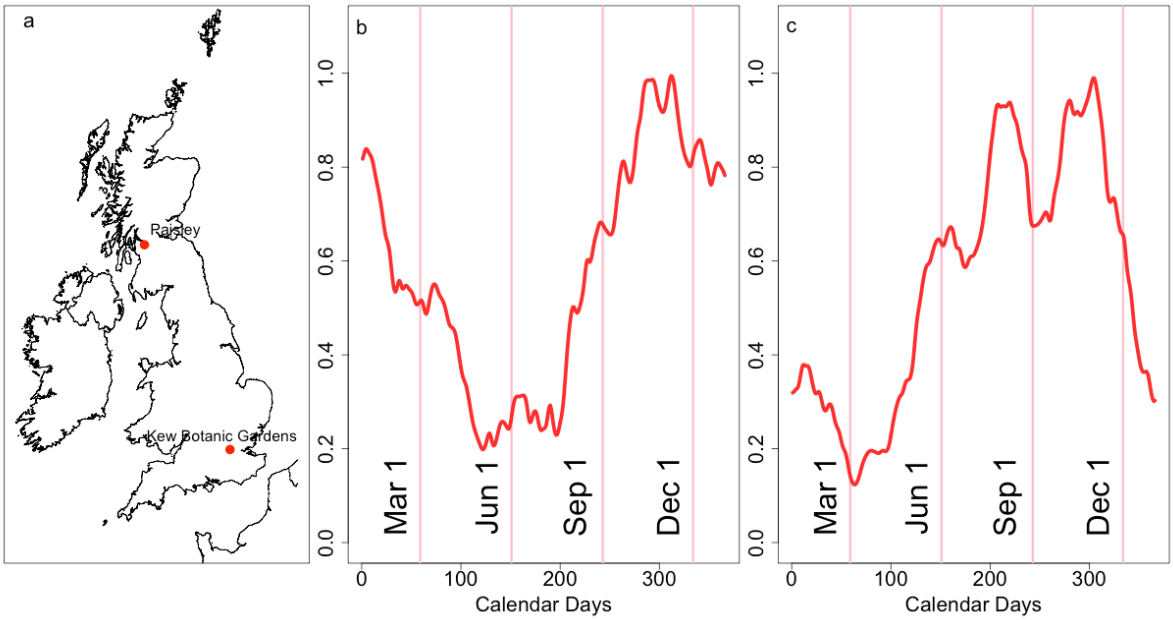

Figure 2 : Relative frequency of Q95 rainfall per day of the year for locations shown in (a), at (b) Paisley; and (c) Kew Royal Botanic Gardens. Vertical lines indicate the first day of the season.

While seasonality is readily visualised in a horizontal manner relative to the calendar day, as in Figure 2, comparisons between years and seasons may benefit from a rotated seasonal approach (Robson, 1999). If θ represents the angular position of the calendar day (at noon) in radians, JDN the Julian day number of the event and LENYR the length of the year (assumed to be 365.25):

$$\theta = (JDN - 0.5)\frac{2\pi}{LENYR} \tag{7}$$

then for N events at i stations, the centroid of all events, $\overline{\theta}$, can be calculated from Equation (8). $\overline{\theta}$ is approximately equal to the calendar day of the greatest peak in extreme event occurrence, while $\overline{r}$ reflects the relative distribution of events throughout the year, with multimodal seasonality shown by $\overline{r} \to 0$ and unimodal seasonality by $\overline{r} \to 1$.

$$\overline{x} = \frac{1}{n}\sum_{i=1}^{N}\cos\theta_i \qquad \overline{y} = \frac{1}{n}\sum_{i=1}^{N}\sin\theta_i$$

$$\overline{r} = \sqrt{\overline{x}^2 + \overline{y}^2} \tag{8}$$

$$\overline{\theta} = \begin{cases} \tan^{-1}\dfrac{\overline{y}}{\overline{x}} & \overline{x} \geq 0 \quad \overline{y} \geq 0 \\ \tan^{-1}\dfrac{\overline{y}}{\overline{x}} + \pi & \overline{x} < 0 \\ \tan^{-1}\dfrac{\overline{y}}{\overline{x}} + 2\pi & \overline{y} < 0 \end{cases}$$

Spatial differences in the seasonal behaviour of daily precipitation extremes are well represented by the regionally pooled maxima, with specific locational responses ably captured by atmospheric and oceanic covariates (e.g. Maraun *et al.*, 2011; Serinaldi and Kilsby, 2012). Smoothing functions within the VGAMs applied to the covariates will reduce the effective contribution of insignificant parameters to zero, and so allow a common model for all regions to be constructed rather than several location specific models. Various measures of temperature and atmospheric circulation were selected *a priori* for inclusion as covariates in the model to describe extreme daily precipitation frequency and intensity, as these variables are well-simulated by climate models (Christensen *et al.*, 2007); this will be beneficial for future iterations of the statistical models which may then be used to project changes to properties of extreme precipitation with greater accuracy than is currently achievable using the outputs from climate models alone (Fowler and Ekström, 2009).

7.1.2 Oceanic-Atmospheric Drivers

A literature search of the drivers of UK extreme daily precipitation recommended the use of either monthly NAO indices, coincident with the month of the event, or a seasonal counterpart (Wilby *et al.*, 2002; Fowler and Kilsby, 2003b; Allan *et al.*, 2009). However, sub-seasonal NAO indices may be more descriptive of the immediate weather rather than large-scale atmospheric patterns (Hurrell and Deser, 2009). Accordingly, a set of seasonal indices combining the most common winter (DJFM; Hurrell, 1995) and summer (JJA; Folland *et al.*, 2009) indices with a spring index comprising April-June and an autumn index of September-October was also examined. The November NAO index was found to be more closely aligned with the winter index (Rodriguez-Fonseca and De Castro, 2002) and so was included in the winter aggregate (normally DJFM only).

Other authors have found strong correlations between monthly SSTs and daily precipitation frequency and intensity in the south of the UK (Phillips and McGregor, 2002). SST and SLP lagged by up to 6 months and SST anomalies over a wider Atlantic region have also be shown to be effective predictors of summer stream flow (Wilby *et al.*, 2002). A strong seasonal pattern in the frequency of UK extreme precipitation events, peaking in the summer or early autumn, suggests that daily air temperature range must play a key role in the onset of extreme precipitation events, as the peak event frequency is coincident with maximum air temperatures. Monthly maximum daily air temperature range was selected as a potential covariate to minimise the noise introduced by using daily temperature measurements. It should be noted that in reality daily air temperature measures means are a cofactor with

extreme precipitation, as large differences in air temperature between the surface and further aloft lead to the onset of precipitation, but precipitation also reduces the surrounding air temperature.

7.1.3 Initial covariate selection

The covariates examined for importance in the regional VGAMs are listed in Table 1.

Covariate	Term	Definition	
Year	T_t		where t is the event index
Day of the year	d_t		
Seasonality: sine	S_{kt}	$\sin(dt')$	$t' = 2\pi t / 365.25$
Seasonality: cosine	C_{kt}	$\cos(dt')$	$t' = 2\pi t / 365.25$
Event intensity	r_t	x_t-u	Where x_t is daily total
Event occurrence	y_t	y_t=1	When $x_t \geq$u (y_t=0, otherwise)
NAO index	N_t		N_t monthly or seasonal
Sea Surface temperature	SS_t		SS_t coincident or ≤ 6 months lag
Normalised mean sea level pressure	SP_t		SP_t coincident or ≤ 6 months lag
Monthly max air temperature	Θ_{TX}		Grid box average maximum
Monthly min air temperature	Θ_{TN}		Grid box average minimum
Monthly maximum range	Θ_{DR}	$\Theta_{TX} - \Theta_{TN}$	

Table 1 : Terms used in the Vector Generalized Additive Models

VGAMs were applied to regionally pooled daily extreme precipitation observations to enhance the reliability of frequency and intensity estimates through the use of larger data sets. Individual station maxima were considered independent when separated by an interval ≥1day between successive events, selecting the maximum of any wet spell (i.e. sequence of two or more wet days). Although it is likely that one storm will be recorded by several stations within each regional pool, either on the same or a consecutive day, using repeated events does not increase the bias in estimates of rate or magnitude, even though there is an increase in the standard error estimate (Hosking, 1990; Morton and Henderson, 2008). The extreme value distribution models for event intensity were standardised by the station median Annual Maximum value, to adjust for inhomogeneity arising from orographic differences, prior to fitting regional GEV distributions. A combined process model was adopted to model the frequency of Q95 events (Poisson) and magnitude (GEV applied to AMAX) for each region.

7.2 Model construction

Penalized maximum likelihood methods for parameter estimation, which are the default option in the computer software (Yee, 2011), were used to fit a Poisson VGAM for frequency and GEV VGAM for intensity for each region. Penalized maximum likelihood is computationally efficient and highly flexible in the selection of model parameters (Wood,

2000), and the resultant model simplicity aids model parameter interpretation. To achieve a suitable balance between model over-fitting and excessive parsimony, the maximum model effective degrees of freedom (edf) are specified and so dictate the response of the term, with edf=1 representing a linear response; the default minimum in VGAM is edf=3 (Yee, 2011). Modified vector backfitting to fit the smooth functions, where $f(x_t)$ is decomposed into linear and non-linear components, improves model convergence rate and numerical stability (Yee, 2011) and was adopted here.

Cubic regression splines were used to fit the smoothed parameters as these outperformed more complex options, such as polynomial splines, in efficiency and efficacy. Complexity was gradually increased from simple models of the response, y_i, against individual explanatory variables to combinations of several covariates, selecting those which explained the highest proportion of variability. Model terms were combinations of those listed in Table 1, tested for suitability through measures such as the model deviance statistic, the Akaike Information Criterion (AIC; Akaike, 1974), and the significance of the correlation with precipitation frequency. In deriving a parsimonious, yet representative, model Wood and Augustin (2002) suggest that a covariate term should be dropped from the model when the following criteria are satisfied:

- the term edf is close to its lower limit;
- the confidence region for the smooth contains zero everywhere;
- removing the term reduces the deviance statistic.

As stepwise iteration to reject unnecessary covariates (Hastie and Tibshirani, 1990) is time consuming, particularly when many covariates are involved, a modified approach was used where only the significant terms from less complex models were included in later multivariate models. Parameter link functions were selected automatically to ensure that the Poisson arrival rate, $\Lambda > 0$, and GEV parameters for location, $\mu > 0$, scale, $\sigma > 0$ and shape, $\xi > -0.5$ (Mestre and Hallegatte, 2009); log-link was used to maintain model stability through avoiding numerical problems associated with negative rate or shape parameters (Yee, 2010). Parameter definitions for the Poisson-GEV model were initially established from $X_1,\ldots,X_q$ covariates as Equation 6.

Although over-dispersed event frequency could be represented with a negative-binomial distribution (Lang, 1999), a Poisson distribution with time-varying rate parameter was considered more representative of the physical processes driving event occurrence

(Chavez-Demoulin and Davison, 2005). Allowing the arrival rate to vary reflects the independence of the maxima and their non-identical distribution throughout the year.

Most regional models were fitted to a sub-set of stations covering the full record period, 1961-2009, to minimise the influence of varying numbers of stations per year in the pool. The only exceptions were Humber (HUM) and Mid Wales (MW) where, due to the low number of observation stations in each region, the whole data pool was employed to construct the models.

7.3 Covariate Selection

The results indicated that the SST one month prior to an event (Lag 1) is more powerful as a covariate than coincident SST, while the coincident monthly NAO index was found to be more important than its seasonal counterpart in all regions. The 6-month lag normalised SLP was a powerful covariate in the bivariate model, but detracted from model performance in combination with any other covariate and so was removed; the information provided from SLP was also replicated by including the monthly NAO. The importance of air temperature metrics also varied between regions, with the maximum monthly air temperature range most frequently achieving the lowest deviance scores and highest model significance. Seasonality as a rotated statistic (Robson, 1999) was statistically better than the simple calendar day covariate, but was found to represent the seasonal cycle poorly and severely increased the computational demand. Consequently, the simpler calendar day representation of seasonality was adopted as a covariate in the final model in preference to the sinusoidal parameter. Finally, the year of occurrence was replicated by inter-annual fluctuations in the other covariates and so was not incorporated in the models.

To achieve the best data representation, whilst minimising measures such as the deviance statistic or AIC and, therefore, maximising model parsimony, each covariate was also tested for its relative degree of flexibility. The modelled smooth terms indicated that only SST required a fully flexible representation, i.e. $f_2\left(ST1_t\right)$; while the relationship with calendar day was semi-flexible using a piece-wise linear regression spline $f_1\left(d_t\right)$ and other terms were represented by a linear relationship with event frequency (NAO and Θ_{DR}). While there is evidence that allowing the scale parameter to depend on covariates improves the distribution fit (e.g. Mestre and Hallegate, 2009; Chavez-Demoullin and Davison, 2005), the fully flexible model was computationally more expensive with AIC scores showing limited or no improvement in the model. This is similar to Cooley (2009), albeit applied to a

considerably larger data set, who found that allowing the scale parameter to be flexible introduces unnecessary complexity for limited computational gain. To minimise computational instability and maintain a degree of parsimony in the VGAM, σ was also modelled as an intercept only term.

7.4 Final Model Selection

Statistical testing of the VGAM model using the four covariate model, which achieved the lowest deviance and AIC scores, against a more parsimonious model, dependent only on d_t and ST_1, suggested that the difference between the models was negligible and the simpler model should be selected. However, a subjective review of data representation is an important part of model selection (Villarini and Serinaldi, 2011), and this indicated that the higher parameter model was more representative of event frequency. The final model includes a combination of flexible, semi- and fully-linear covariates. The variables selected for their explanatory power of event frequency and magnitude in all regions are: day of year (d_t), monthly NAO index (N_t), lagged monthly SST ($ST1_t$) and monthly maximum air temperature range (Θ_{DRt}). Air temperature will be particularly beneficial for adaptation planning using climate projections, as confidence in projections of this variable are much higher than for extreme daily precipitation (Christensen *et al.*, 2007; Fowler and Ekström, 2009). Known relationships with seasonality and the NAO may also aid seasonal forecasting and planning by improving the probability of accurately forecasting one or more extreme events in the year. The selected model may also be more sensitive to future changes in extreme precipitation through the inclusion of two different temperature terms, which tend to be better represented within Global Circulation Models (GCM) and Regional Climate Models (RCM; Hegerl and Zwiers, 2011).

The Poisson model was fitted first to represent event frequency and followed by the GEV model, using the same covariates for the GEV model as for the Poisson model; this approach aids model interpretation. The final model form for both Poisson and GEV distribution model parameters are described in Equation 7 and parameter estimates can be found in Table 2:

$$
\begin{aligned}
&\log \Lambda(x) = \beta_{0(1)} + f_{1(1)}(d_t) + f_{2(1)}(ST1_t) + \beta_{3(1)} N_t + \beta_{4(1)} \Theta_{DRt} \\
&\mu(x) = \beta_{0(2)} + f_{1(2)}(d_t) + f_{2(2)}(ST1_t) + \beta_{3(2)} N_t + \beta_{4(2)} \Theta_{DRt} \\
&\log \sigma(x) = \beta_{0(3)} \\
&\log\left(\xi(x) + \frac{1}{2}\right) = \beta_{0(4)}
\end{aligned}
\tag{9}
$$

Seasonality, d_t, was found to be the most important covariate for most regions and models, explaining between 45-90% of the variability in event frequency; the next most important variable was monthly maximum air temperature range , Θ_{DRt}, followed by lagged monthly SST, $ST1_t$, or monthly NAO index, N_t (dependent on location). Calendar day and air temperature jointly encompass the twin seasonality in event frequency observed in several regions as air temperature is, perforce, seasonally driven. Air temperature range was more important than the calendar day in explaining extreme precipitation event frequency in south eastern regions, which tend to receive more summertime convective storms driven by temperature gradient. Similarly, SSTs and NAO differ in importance between regions, displaying a north-south divide whereby the explanatory power of the NAO was greatest in northern and Atlantic facing regions, while SST dominated in south and eastern regions.

Figures 3 and 4 are examples of the smoothing functions which were fitted to each regional Poisson and GEV VGAM but shown here only for the Northern Ireland (NI) region; ±2 standard error bars are indicated by dashed lines. The strong seasonality observed in both the frequency and magnitude of events is well replicated by the model seasonality, d_t. The linear term for air temperature range is indicative of a negative correlation between air temperature range and event magnitude or frequency, which is consistent with observations in this region of the most intense precipitation during the summer when the diurnal temperature range is at its lowest (Zhou *et al.*, 2009). Event frequency has a positive correlation with lagged SST for all regions. However, the SST relationship is less well defined in the GEV model, where southern regions show a positive correlation between North Atlantic SST and extreme precipitation event intensity but there is a more variable relationship in northern and Atlantic facing regions.

Region	Estimated Model Terms											
	Poisson					Generalized Extreme Value						
	$\log\Lambda$					μ					σ	ξ
	β_0	$\mathbf{d_t}$	$\mathbf{ST1_t}$	$\mathbf{N_t}$	$\boldsymbol{\theta_t}$	β_0	$\mathbf{d_t}$	$\mathbf{ST1_t}$	$\mathbf{N_t}$	$\boldsymbol{\theta_t}$	$\exp(\beta_0)$	$\exp(\beta_0)-0.5$
NHI	-1.90	**-1.04**	0.10	0.21	-0.20	0.81	**-0.11**	$2.0e^{-2}$	$-2.5e^{-2}$	$-1.8e^{-2}$	0.22	0.13
ES	-0.57	-0.23	0.01	0.05	**-0.28**	0.76	**0.67**	$2.3e^{-2}$	$-2.7e^{-2}$	$-3.5e^{-2}$	0.23	0.13
FOR	-0.88	**0.84**	0.03	0.07	-0.34	0.94	**0.12**	$1.2e^{-2}$	$-2.8e^{-2}$	$-3.1e^{-2}$	0.25	0.03
SH	-0.64	**-1.07**	0.03	0.25	-0.28	0.93	**-0.17**	$2.2e^{-4}$	$-2.9e^{-3}$	$3.0e^{-3}$	0.21	0.03
NW	-1.20	**0.47**	0.03	0.08	-0.23	0.92	**0.12**	$6.9e^{-5}$	$-1.0e^{-2}$	$-5.2e^{-3}$	0.23	0.09
NE	-2.91	**0.85**	0.16	-0.14	-0.28	1.06	**-0.19**	$7.9e^{-3}$	$-3.7e^{-2}$	$-3.5e^{-2}$	0.25	0.07
HUM	-3.25	**2.39**	0.05	-0.19	-0.24	1.09	**-0.38**	$-2.2e^{-3}$	$-3.2e^{-2}$	$-1.5e^{-2}$	0.25	0.08
EA	-2.86	**4.69**	0.07	-0.06	-0.25	0.84	$4.2e^{-2}$	$1.9e^{-3}$	**-0.05**	$-7.2e^{-4}$	0.25	0.06
SE	-2.54	**3.37**	0.10	-0.02	-0.31	0.67	**0.39**	$6.2e^{-3}$	$-9.1e^{-3}$	$6.3e^{-3}$	0.21	0.16
WC	-2.07	**1.43**	0.06	-0.03	-0.24	0.71	**-0.07**	$2.2e^{-2}$	$-1.5e^{-2}$	$-9.7e^{-3}$	0.21	0.04
MW	-2.09	**2.47**	0.01	0.17	-0.29	1.17	**0.51**	$-1.9e^{-2}$	$-1.6e^{-2}$	$-2.5e^{-2}$	0.21	0.09
SOL	-0.85	-0.23	0.02	0.18	**-0.27**	1.01	**0.15**	$-5.1e^{-4}$	$-1.0e^{-3}$	$-1.7e^{-2}$	0.19	0.14
SW	-1.48	**0.93**	0.06	0.01	-0.26	0.51	**0.14**	$2.8e^{-2}$	$3.0e^{-3}$	$9.0e^{-3}$	0.21	0.10
NI	-2.21	-0.15	0.10	-0.03	**-0.20**	1.01	**0.04**	$-1.2e^{-3}$	$-2.0e^{-2}$	$-1.6e^{-2}$	0.21	0.13

Table 2 : Contributions of atmospheric variables (model term covariates) to distribution parameters, with the most influential covariate highlighted in bold for each extreme rainfall region.

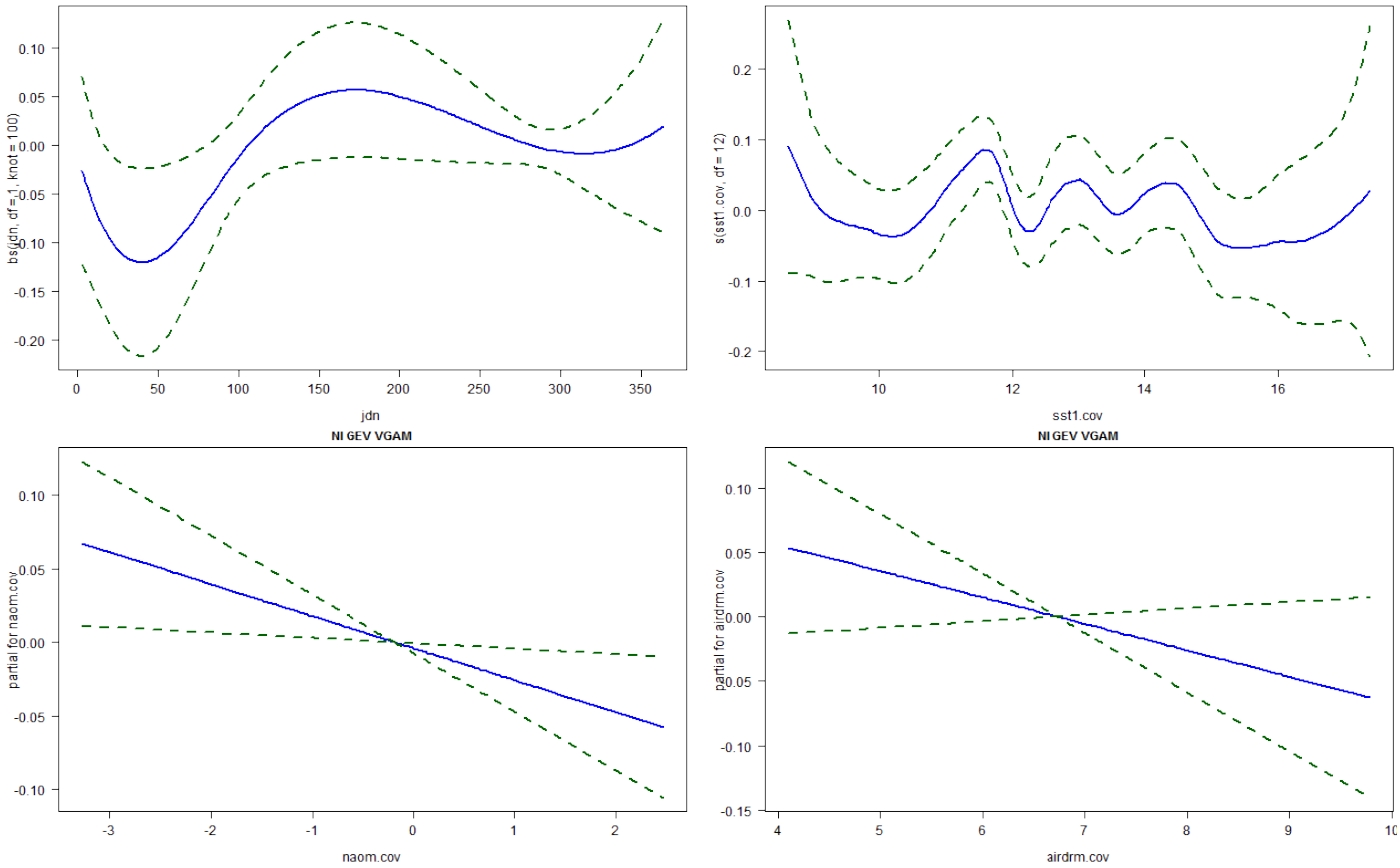

Figure 3 : Generalized Extreme Value VGAM fitted to the Northern Ireland Region annual maxima precipitation to model event intensity. Lagged SST (sst1.cov) has 12 degrees of freedom (edf), day of year (jdn) is piece-wise linear centred about a knot at days 100 and 300 and edf=12, NAO (naom.cov) and

monthly air temperature range (airdrm.cov) are both linear. The *dashed lines* are ±2 SE bands. From top left going clockwise, the fitted functions are $\widehat{\beta}(d_t), \widehat{f_{1(1)}}(ST1_t), \widehat{\beta}\Theta_t, \widehat{\beta}N_t$

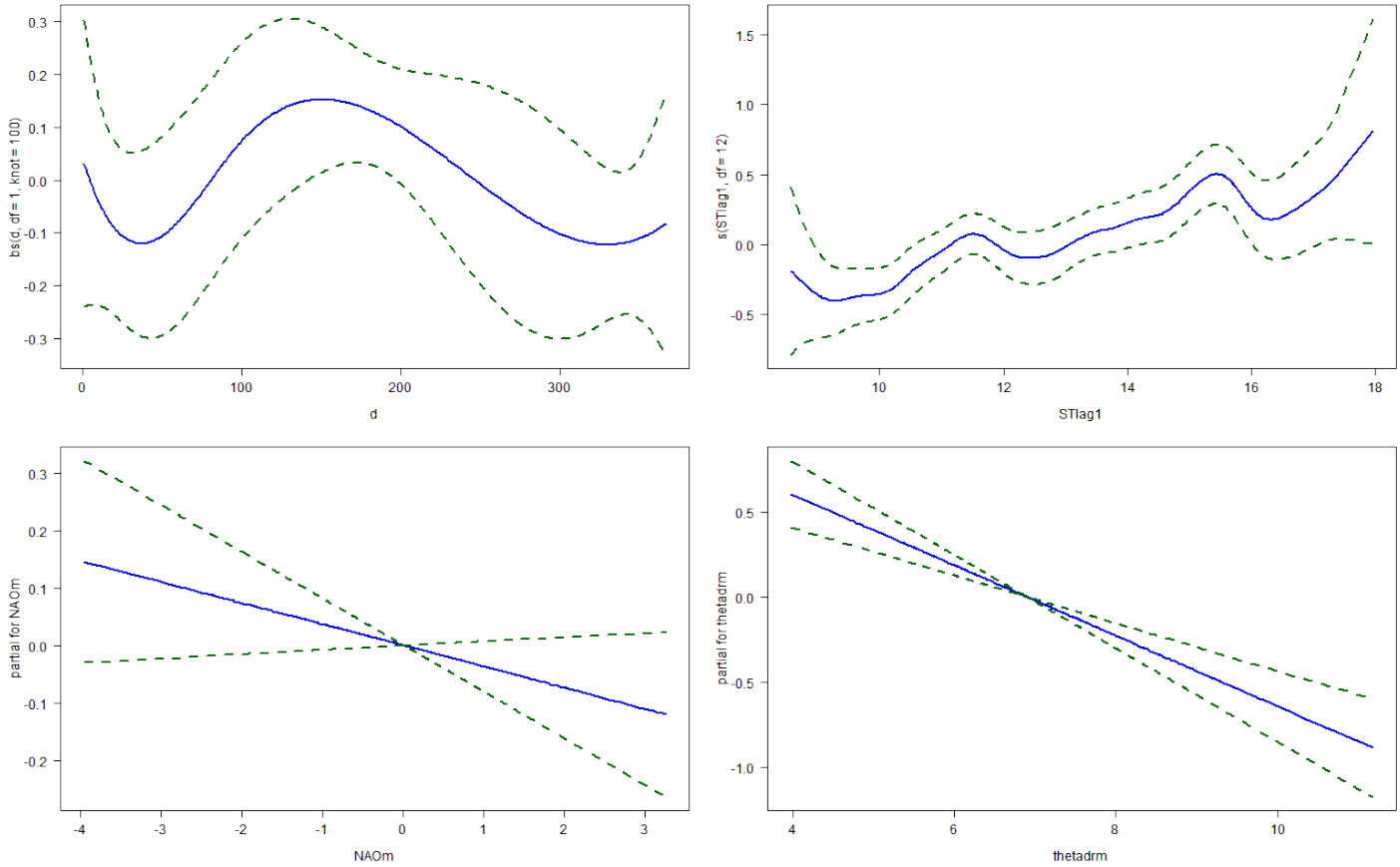

Figure 4 : Poisson VGAM fitted to the Northern Ireland Region Q95 precipitation to model event frequency. The terms are a combination of smoothed, piece-wise linear and fully linear functions as for the GEV VGAM. The *dashed lines* are ±2 SE bands. From top left going clockwise, the fitted functions are $\widehat{\beta}(d_t), \widehat{f_{1(1)}}(ST1_t), \widehat{\beta}\Theta_t, \widehat{\beta}N_t$

8 Model Validation

Hypothesised changes in event seasonality, frequency and intensity should not be examined if the observed base distribution is modelled incorrectly. Therefore, the ability of each regional combined process model to represent observed extreme daily precipitation event frequency (the Poisson models) and magnitude (the GEV models) throughout the year was checked by simulating a large number of events from each VGAM distribution. Visual tools such as quantile-quantile plots and comparisons of the model outputs with observed data were then used to verify the model's adequacy, before examining inter-annual patterns in extreme precipitation frequency.

8.1 Event frequency and seasonality

Figure 5, column 1, compares the frequency of observed events per day of year with the simulated frequency using covariate data for the same period of record (1961-2000) for 5 regions, which are representative of the results from the other nine regions. The two

frequency densities match well without excessive reproduction of day to day variability, which would suggest an over-fitted model (Wood, 2006), attaining maximum and minimum frequency in the correct periods. The permitted degree of flexibility in the models result in most regions replicating the observed multiple peaks and regional variations in the timing of event frequency, which arise from the interaction and changing importance of the covariates throughout the year. Two regions which are less well represented by the model, MW (not shown) and HUM, were derived from smallest data sets; each having fewer than five stations with complete records from 1961 to 2009. While the minimum frequency density is underestimated in the two regions, the model simulates the correct timing, duration, and magnitude of maximum and minimum event frequencies.

Each VGAM produced a sequence of daily Poisson rate parameter estimates, dependent on the relevant covariate data from which a median distribution for the year could also be derived. Multiple draws from the simulated distributions were required to objectively characterise the variability of observed extreme event frequency, and to replicate the randomness with which events may occur given different driving atmospheric conditions. The quantile-quantile plots depicted in Figure 5, column 2, are derived from the standardised distributions of observed frequency against standardised frequencies simulated from 500 random draws. These show good correlation between the observed and simulated distribution quantiles for most regions; a few regions (e.g. FOR, NHI) are less well represented at the lower tail of event frequency. As these regions tend to be dominated by the influence of the North Atlantic Oscillation on storm occurrence and intensity, it is likely that the discrepancies have arisen through the model tendency towards SST flexibility rather than towards the NAO index.

8.2 Intensity

A similar exercise was carried out for the regionally standardised annual maxima, sampling from the fitted GEV-VGAMs 500 times to establish a range of possible event magnitudes. Figure 5, column 3, illustrates the quantile-quantile plots obtained from the standardised observed AMAX vs. maxima sampled from the GEV distribution; these regional plots are generally representative of the observed maxima. As with the Poisson model, the largest one or two maxima are not well represented by one or two regional models which show under- or over-estimated maxima (e.g. FOR) but, for the most part, the simulated and observed quantiles lie within expected confidence bounds. A likely cause of the discrepancies is the use of a homogeneously applied model, which does not apply preferential weighting to

covariates in different regions. The disparate nature of station observations within some larger regions, such as NHI, where lack of data precluded further regional sub-division, also has an impact on the regional model fit. The latter may be resolved when regional boundary definitions are improved with additional station information. In contrast, introducing regional weights on different covariates would augment the model complexity as accurate representation would require the weighting to vary temporally in response to different covariate combinations. The potentially limited return for such an increase in complexity and computational cost was not considered worthwhile.

Annual return period magnitudes were also estimated from the simulated model quantiles for each region, using covariate data for 1961-2000, and compared to return period magnitudes calculated for observed annual maxima (Figure 5, column 4). The shape and steepness of each estimated distribution curve compares well with those for the observed annual maxima, providing reassurance that the model is adequate in its representation of event return frequency and magnitude.

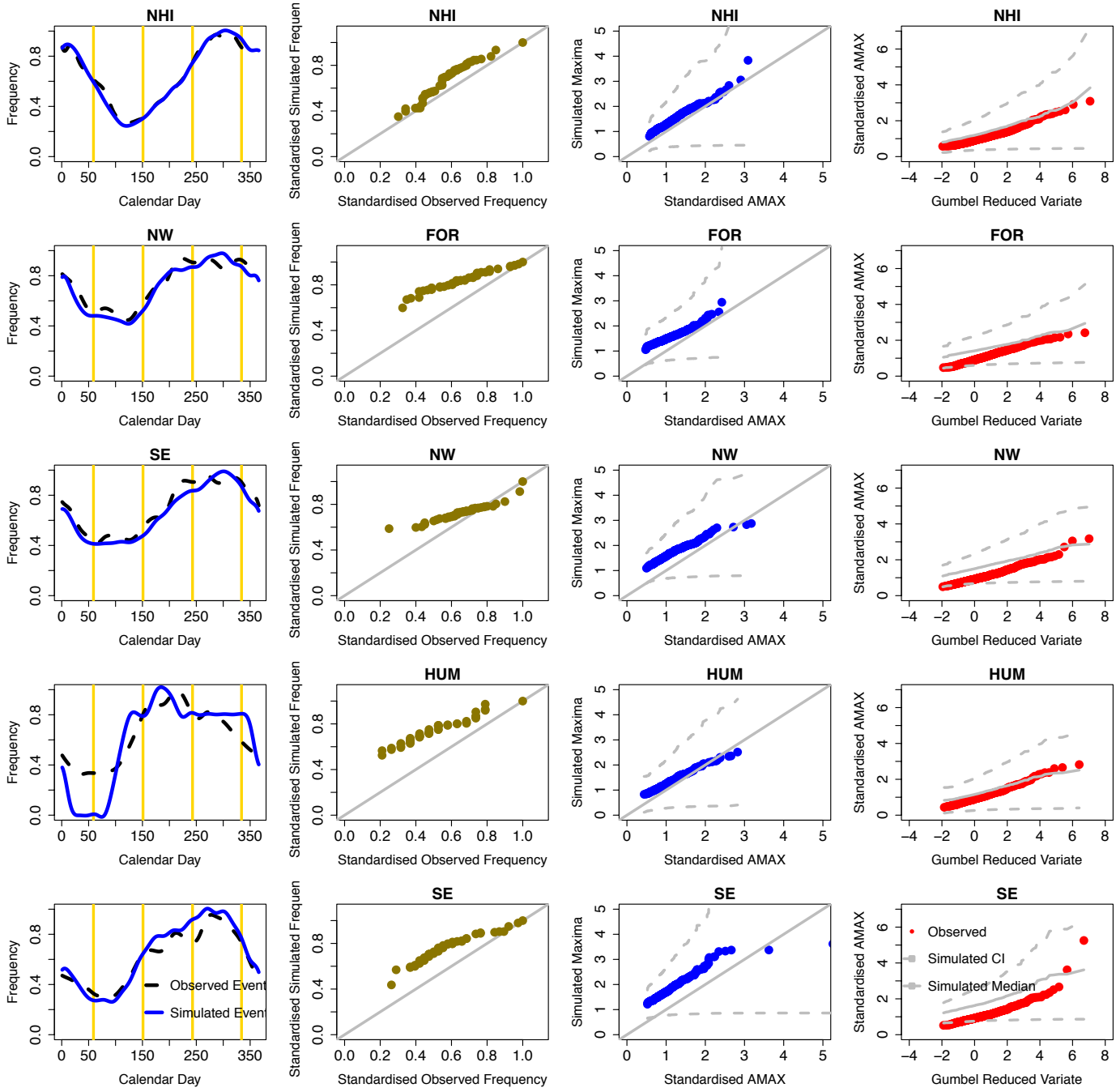

Figure 5 : Comparison of Observed and Simulated results from: the Poisson VGAM for mean event frequency per day of year (Column 1); quantile-quantile plots (Column 2) ; quantile-quantile plots of the GEV VGAM for event magnitude (Column 3) and estimated annual return period magnitudes (Column 4).

9 Conclusions

Allowance for non-stationarity in regional precipitation or flood estimates has been addressed by the research community, but is currently far from common practice (Jakob *et al.*, 2011); most analyses of extreme precipitation have focussed on traditional extreme value analyses to estimate the likely return frequency of specific events (Ghil *et al.*, 2011). This article has presented a new approach to accommodate non-stationarity in frequency and

magnitude estimates of extreme daily precipitation by using spatially pooled data to examine seasonality. Allowing the parameters to vary temporally, in response to external covariates, represents the non-identically distributed nature of precipitation maxima over the course of the year. A Vector Generalized Additive Model for Poisson and GEV distributions, dependent on external covariates such as sea surface temperature, was developed to allow for the non-stationarity in observed event intensity and frequency and to assess apparent changes in the distributions; this is an effective method to abandon the stationarity paradigm (Milly *et al.*, 2008; Lins and Cohn, 2011). Fitting a statistical model to observed data enabled the use of observed atmospheric and meteorological conditions to simulate event probability many hundred times and examine hypothesised changes to event frequency or 'clustering' over long time periods, including the recent decade. Data limitations prescribed a non-standard approach, combining the Poisson and GEV distributions to model frequency and intensity rather than the orthogonal point process using Poisson and GP distributions. It is not considered to have had a detrimental effect on the statistical models for UK extreme precipitation produced here. However, in locations where there is a marked difference between the wet and dry seasons this approach may not be so valid; selecting the single largest daily rainfall total per year reduces the available information for covariate selection and consequently affects the model fit. The GP distribution, fitted with a seasonally varying threshold (Coelho *et al.*, 2008) may prove a more informative model if sufficient POT maxima are available.

The benefit of using a VGAM rather than linear modelling was the resultant parameter flexibility, allowing for temporal variation throughout the year with respect to multiple influences. GAMs have rarely been applied to hydrological series, and the extension to extreme value distributions through VGAMs has seldom been applied to daily precipitation extremes, making this a novel analysis of extreme precipitation.

The contribution of each covariate to the estimated parameters confirmed that seasonality, represented by calendar day, is the principal driver of daily extreme precipitation event frequency in the UK, with monthly maximum daily air temperature range having the second most importance. Calendar day and air temperature jointly encompass the twin seasonality in event frequency observed in several regions as air temperature is, perforce, seasonally driven. SSTs and NAO differ in importance between regions, displaying a north-south divide with northern Atlantic regions dominated by the NAO and south eastern regions by SSTs.

A negative relationship exists between monthly air temperature range and both event frequency and magnitude. This parallels the observed relationship between the frequency and magnitude of summer convective events (Zhou *et al.*, 2009) and confirms that the probability of extreme precipitation is higher, and events are more likely to be intense, during times of elevated temperature when the diurnal temperature range is at its lowest. Climate projections suggest that increases in global mean temperature will also bring about a reduction in diurnal air temperature range (Christensen *et al.*, 2007); a trend which is already seen in many regions in observations (Jenkins *et al.*, 2010). In combination with the positive relationship found with SSTs, this implies that UK short duration (daily) precipitation extremes will increase in frequency and intensity with increases in global mean temperature, confirming hypotheses derived from physical processes about the nature of future extreme precipitation (Trenberth, 2011).

Poisson models based on VGAM parameters were able to replicate observed event frequency well, without over-fitting the model; regional GEV-VGAM models reproduced event maxima satisfactorily. There are minor differences between the relative importance of the covariates in each of the models, which may have arisen from the non-standard approach combining Poisson and GEV distributions. It should be noted that the point process approach is potentially a more powerful technique which, if it had been feasible to apply, might have clarified the relationship between extreme responses and their drivers and so minimised these differences between the models. Simulating from these statistical models of event probability, in conjunction with known atmospheric or meteorological conditions, it will now be possible to establish whether apparent changes in observed extreme behaviour response arise from climatic regimes or represent a longer term trend. The final model includes two different temperature terms, which tend to be better represented within GCMs and RCMs (Hegerl and Zwiers, 2011), and so it may be more effective in deriving the likely future changes in extreme precipitation than direct modelling approaches. Assuming that GCMs or RCMs can adequately reproduce the VGAM model covariates, for instance atmospheric indices such as the NAO are notoriously difficult due to their shifting centre of action (Stephenson *et al.*, 2006), it should, therefore be possible to extend the research to determine the approximate magnitude of changes to the frequency and intensity of extreme precipitation under future climate conditions.

Statistical downscaling from regional climate models would benefit from these improvements to the characterisation of UK extreme precipitation and could be used to assess

likely future changes in hydrological responses. Comparing the results presented in this article with those obtained from climate projections for the control period would be of interest to understand discrepancies in the current representation of both the physical processes driving extreme precipitation in climate models and the simulation of extreme precipitation itself.

10 References

Akaike, H., 1974, A new look at the statistical model identification. *IEEE Transactions on Automatic Control,* 19:716–723.

Alexander, L. V, Zhang, X., Peterson, T.C., Caesar, J., Gleason, B., Klein Tank, A.M.G., Haylock, M., Collins, D., Trewin, B., Rahimzadeh, F., Tagipour, A., Rupa Kumar, K., Revadekar, J., Griffiths, G., Vincent, L., Stephenson, D.B., Burn, J., Aguilar, E., Brunet, M., Taylor, M., New, M., Zhai, P., Rusticucci, M., and Vazquez-Aguirre, J.L., 2006, Global observed changes in daily climate extremes of temperature and precipitation. *J Geophys Res,* 111:D05109. doi:10.1029/2005jd006290.

Allamano, P., Laio, F., and Claps, P., 2011, Effects of disregarding seasonality on the distribution of hydrological extremes. *Hydrol Earth Syst Sci,* 15:3207–3215. doi:10.5194/hess-15-3207-2011.

Allan, R., and Ansell, T., 2006, A New Globally Complete Monthly Historical Gridded Mean Sea Level Pressure Dataset (HadSLP2): 1850–2004. *Journal of Climate,* 19:5816–5842. doi:10.1175/jcli3937.1.

Allan, R., Tett, S., and Alexander, L., 2009, Fluctuations in autumn-winter severe storms over the British Isles: 1920 to present. *International Journal of Climatology,* 29:357–371.

Ammann, C.M., Joos, F., Schimel, D.S., Otto-Bliesner, B.L., and Tomas, R.A., 2007, Solar influence on climate during the past millennium: Results from transient simulations with the NCAR Climate System Model. *Proceedings of the National Academy of Sciences,* 104:3713–3718.

Casty, C., Wanner, H., Luterbacher, J., Esper, J., and Böhm, R., 2005, Temperature and precipitation variability in the European Alps since 1500. *International Journal of Climatology,* 25:1855–1880. doi:10.1002/joc.1216.

Chavez-Demoulin, V., and Davison, A.C., 2005, Generalized additive modelling of sample extremes. *Journal of the Royal Statistical Society: Series C (Applied Statistics),* 54:207–222. doi:10.1111/j.1467-9876.2005.00479.x.

Christensen, J.H., Hewitson, B., Busuioc, A., Chen, A., Gao, X., Held, I.M., Jones, R., Kolli, R.K., Kwon, W.-T., Laprise, R., Magana Rueda, V., Mearns, L.O., Menendez, C.G., Raisanen, J., Rinke, A., Sarr, A., and Whetton, P., 2007, Regional Climate Projections. In: Solomon S, Qin D, Manning M, Chen Z, Marquis M, Averyt KB, Tignor M, Miller HL (eds) *Climate Change 2007: The Physical Science Basis. Contribution of Working Group I to the Fourth Assessment Report of the Intergovernmental Panel on Climate Change*. Cambridge University Press, Cambridge, UK,.

Coelho, C.A.S., Ferro, C.A.T., Stephenson, D.B., Steinskog, D.J., 2008, Methods for Exploring Spatial and Temporal Variability of Extreme Events in Climate Data. *Journal of Climate*, 21, pp.2072–2092. 10.1175/2007JCLI1781.1

Cohn, T.A., and Lins, H.F., 2005, Nature's style : Naturally trendy. *Geophysical research letters,* 32:23402.1–23402.5.

Coles, S., 2001, An Introduction to Statistical Modeling of Extreme Values. Springer-Verlag, Berlin.

Colman, A., 1997, Prediction of summer central England temperature from preceding North Atlantic winter sea surface temperature. *International Journal of Climatology,* 17:1285–1300.

Cooley, D., 2009, Extreme value analysis and the study of climate change. *Climatic Change,* 97:77–83. doi:10.1007/s10584-009-9627-x.

Coumou, D., and Rahmstorf, S., 2012, A decade of weather extremes. *Nature Climate Change,* 2:1–6. doi:10.1038/nclimate1452.

Davison, A.C., and Smith, R.L., 1990, Models for Exceedances over High Thresholds. *Journal of the Royal Statistical Society Series B (Methodological),* 52:393–442.

Della-Marta, P., Luterbacher, J., Von Weissenfluh, H., Xoplaki, E., Brunet, M., and Wanner, H., 2007, Summer heat waves over western Europe 1880–2003, their relationship to large-scale forcings and predictability. *Climate Dynamics,* 29:251–275. doi:10.1007/s00382-007-0233-1.

Eastoe, E.F., and Tawn, J.A., 2010, Statistical models for overdispersion in the frequency of peaks over threshold data for a flow series. *Water Resour Res,* 46:W02510. doi:10.1029/2009wr007757.

Faraway, J.J., 2006, Extending the linear model with R: generalized linear, mixed effects and nonparametric regression models. Chapman & Hall/CRC.

Fawcett, L., and Walshaw, D., 2007, Bayesian inference for clustered extremes. *Extremes,* 11:217–233. doi:10.1007/s10687-007-0054-y.

Folland, C.K., Knight, J., Linderholm, H.W., Fereday, D., Ineson, S., and Hurrell, J.W., 2009, The Summer North Atlantic Oscillation: Past, Present, and Future. *Journal of Climate,* 22:1082–1103. doi:10.1175/2008jcli2459.1.

Fowler, H., Cooley, D., Sain, S., and Thurston, M., 2010, Detecting change in UK extreme precipitation using results from the climateprediction.net BBC climate change experiment. *Extremes,* 13:241–267. doi:10.1007/s10687-010-0101-y.

Fowler, H.J., and Ekström, M., 2009, Multi-model ensemble estimates of climate change impacts on UK seasonal precipitation extremes. *International Journal of Climatology,* 29:385–416. doi:10.1002/joc.1827.

Fowler, H.J., and Kilsby, C.G., 2003a, A regional frequency analysis of United Kingdom extreme rainfall from 1961 to 2000. *International Journal of Climatology,* 23:1313–1334.

Fowler, H.J., and Kilsby, C.G., 2003b, Implications of changes in seasonal and annual extreme rainfall. *Geophysical Research Letters,* 30:1720–1723.

Furrer, E.M., and Katz, R.W., 2008, Improving the simulation of extreme precipitation events by stochastic weather generators. *Water Resources Research,* 44. doi:10.1029/2008WR007316.

Furrer, E.M., Katz, R.W., Walter, M.D., and Furrer, R., 2010, Statistical modeling of hot spells and heat waves. *Climate Research,* 43:191–205. doi:10.3354/cr00924.

Gershunov, A., and Douville, H., 2008, Extensive summer hot and cold extremes under current and possible future climatic conditions: Europe and North America. In: Diaz H, Murnane R (eds) *Climate Extremes and Society*. Cambridge University Press, pp 74–98.

Ghil, M., Yiou, P., Hallegatte, S., Malamud, B.D., Naveau, P., Soloviev, A., Friederichs, P., Keilis-Borok, V., Kondrashov, D., Kossobokov, V., Mestre, O., Nicolis, C., Rust, H.W., Shebalin, P., Vrac, M., Witt, A., and Zaliapin, I., 2011, Extreme events: dynamics, statistics and prediction. *Nonlin Processes Geophys,* 18:295–350. doi:10.5194/npg-18-295-2011.

Gilleland, E., Katz, R.W., and Young, G.E.T.-1. 6., 2009, extRemes: Extreme value toolkit. http://cran.r-project.org/package=extRemes.

Hastie, T.J., and Tibshirani, R.J., 1990, Generalized Additive Models. Taylor and Francis.

Hegerl, G., and Zwiers, F., 2011, Use of models in detection and attribution of climate change. *Wiley Interdisciplinary Reviews: Climate Change,* 2:570–591. doi:10.1002/wcc.121.

Held, I.M., and Soden, B.J., 2006, Robust Responses of the Hydrological Cycle to Global Warming. *Journal of Climate,* 19:5686–5699. doi:10.1175/JCLI3990.1.

Hosking, J.R.M., 1990, L-Moments: Analysis and Estimation of Distributions Using Linear Combinations of Order Statistics. *Journal of the Royal Statistical Society Series B (Methodological),* 52:105–124.

Hosking, J.R.M. & Wallis, J.R., 1997. *Regional Frequency Analysis: an approach based on L-moments.* Cambridge University Press, Cambridge, UK.

Hurrell, J.W., 1995, Decadal Trends in the North Atlantic Oscillation: Regional Temperatures and Precipitation. *Science,* 269:676–679.

Hurrell, J.W., and Deser, C., 2009, North Atlantic climate variability: The role of the North Atlantic Oscillation. *Journal of Marine Systems,* 78:28–41.

Hyndman, R.J., and Grunwald, G.K., 2000, Applications: Generalized Additive Modelling of Mixed Distribution Markov Models with Application to Melbourne's Rainfall. *Australian & New Zealand Journal of Statistics,* 42:145–158. doi:10.1111/1467-842x.00115.

Jakob, D., Karoly, D.J., and Seed, A., 2011, Non-stationarity in daily and sub-daily intense rainfall - Part 2: Regional assessment for sites in south-east Australia. *Nat Hazards Earth Syst Sci,* 11:2273–2284. doi:10.5194/nhess-11-2273-2011.

Jenkins, G., Perry, M., and Prior, J., 2010, The climate of the UK and recent trends. http://ukclimateprojections.defra.gov.uk/content/view/816/500.

Jones, M.R., Blenkinsop, S., Fowler, H.J., and Kilsby, C.G., 2013, Objective classification of extreme rainfall regions for the UK and updated estimates of trends in regional extreme rainfall. *International Journal of Climatology,* In Press.

Jones, M.R., Fowler, H.J., Kilsby, C.G., and Blenkinsop, S., 2010, An updated regional frequency analysis of United Kingdom extreme rainfall 1961-2009. *BHS 2010: Role of Hydrology in Managing Consequences of a Changing Global Environment*:110–118.

Jones, M.R., Fowler, H.J., Kilsby, C.G., and Blenkinsop, S., 2012, An assessment of changes in seasonal and annual extreme rainfall in the UK between 1961 and 2009. *International Journal of Climatology,* 33(5):1178-1194. doi:10.1002/joc.3503.

Jones, P.D., and Harris, I.E., 2009, CRU Times Series (TS) high resolution gridded datasets. http://badc.nerc.ac.uk/view/badc.nerc.ac.uk__ATOM__dataent_1256223773328276.

Jones, P.D., Jonsson, T., and Wheeler, D., 1997, Extension to the North Atlantic oscillation using early instrumental pressure observations from Gibraltar and south-west Iceland. *International Journal of Climatology,* 17:1433–1450.

Karnauskas, K.B., and Busalacchi, A.J., 2009, The Role of SST in the East Pacific Warm Pool in the Interannual Variability of Central American Rainfall. *Journal of Climate,* 22:2605–2623. doi:10.1175/2008JCLI2468.1.

Katz, R.W., Parlange, M.B., and Naveau, P., 2002, Statistics of extremes in hydrology. *Advances in Water Resources,* 25:1287–1304.

Klein Tank, A.M.G., Wijngaard, J.B., Können, G.P., Böhm, R., Demarée, G., Gocheva, A., Mileta, M., Pashiardis, S., Hejkrlik, L., Kern-Hansen, C., Heino, R., Bessemoulin, P., Müller-Westermeier, G., Tzanakou, M., Szalai, S., Pálsdóttir, T., Fitzgerald, D., Rubin, S., Capaldo, M., Maugeri, M., Leitass, A., Bukantis, A., Aberfeld, R., Van Engelen, A.F. V, Forland, E., Mietus, M., Coelho, F., Mares, C., Razuvaev, V., Nieplova, E., Cegnar, T., López, J.A., Dahlström, B., Moberg, A., Kirchhofer, W., Ceylan, A., Pachaliuk, O., Alexander, L. V, and Petrovic, P., 2002, Daily dataset of 20th-century surface air temperature and precipitation series for the European Climate Assessment. *International Journal of Climatology,* 22:1441–1453. doi:10.1002/joc.773.

Koutsoyiannis, D., 2003, Climate change, the Hurst phenomenon, and hydrological statistics. *Hydrological Sciences Journal,* 48:3–24.

Lang, M., 1999, Theoretical discussion and Monte-Carlo simulations for a Negative Binomial process paradox. *Stochastic Environmental Research and Risk Assessment,* 13:183–200. doi:10.1007/s004770050038.

Li, X., Jiang, F., Li, L., and Wang, G., 2011, Spatial and temporal variability of precipitation concentration index, concentration degree and concentration period in Xinjiang, China. *International Journal of Climatology,* 31:1679–1693. doi:10.1002/joc.2181.

Lins, H.F., and Cohn, T.A., 2011, Stationarity: Wanted Dead or Alive? *JAWRA Journal of the American Water Resources Association,* 47:475–480. doi:10.1111/j.1752-1688.2011.00542.x.

Madsen, H., Pearson, C.P. & Rosbjerg, D., 1997. Comparison of annual maximum series and partial duration series methods for modeling extreme hydrologic events: 2. Regional modeling. Water Resources Research, 33(4), pp.759–769.

Maraun, D., Osborn, T., and Rust, H., 2011, The influence of synoptic airflow on UK daily precipitation extremes. Part I: Observed spatio-temporal relationships. *Climate Dynamics,* 36:261–275. doi:10.1007/s00382-009-0710-9.

Matalas, N.C., 1997, Stochastic Hydrology in the Context of Climate Change. *Climatic Change,* 37:89–101. doi:10.1023/a:1005374000318.

Mestre, O., and Hallegatte, S., 2009, Predictors of Tropical Cyclone Numbers and Extreme Hurricane Intensities over the North Atlantic Using Generalized Additive and Linear Models. *Journal of Climate,* 22:633–648. doi:10.1175/2008jcli2318.1.

Milly, P.C.D., Betancourt, J., Falkenmark, M., Hirsch, R.M., Kundzewicz, Z.W., Lettenmaier, D.P., and Stouffer, R.J., 2008, CLIMATE CHANGE: Stationarity Is Dead: Whither Water Management? *Science,* 319:573–574. doi:10.1126/science.1151915.

Mitchell, T.D., and Jones, P.D., 2005, An improved method of constructing a database of monthly climate observations and associated high-resolution grids. *International Journal of Climatology,* 25:693–712. doi:10.1002/joc.1181.

Moberg, A., and Jones, P.D., 2005, Trends in indices for extremes in daily temperature and precipitation in central and western Europe, 1901-99. *International Journal of Climatology,* 25:1149–1171.

Morton, R., and Henderson, B.L., 2008, Estimation of nonlinear trends in water quality: An improved approach using generalized additive models. *Water Resour Res,* 44:W07420. doi:10.1029/2007wr006191.

Muza, M.N., Carvalho, L.M. V, Jones, C., and Liebmann, B., 2009, Intraseasonal and Interannual Variability of Extreme Dry and Wet Events over Southeastern South America and the Subtropical Atlantic during Austral Summer. *Journal of Climate,* 22:1682–1699. doi:10.1175/2008JCLI2257.1.

Neal, R.A., and Phillips, I.D., 2009, Summer daily precipitation variability over the East Anglian region of Great Britain. *International Journal of Climatology,* 29:1661–1679. doi:10.1002/joc.1826.

Nelder, J.A., and Wedderburn, R.W.M., 1972, Generalized Linear Models. *J R Statist Soc A,* 135:370.

NOAA, 2011, Teleconnection Patterns. http://www.cpc.ncep.noaa.gov/data/teledoc/telecontents.shtml.

Phillips, I.D., and McGregor, G.R., 2002, The relationship between monthly and seasonal South-west England rainfall anomalies and concurrent North Atlantic sea surface temperatures. *International Journal of Climatology,* 22:197–217. doi:10.1002/joc.726.

Pryor, S.C., Howe, J.A., and Kunkel, K.E., 2009, How spatially coherent and statistically robust are temporal changes in extreme precipitation in the contiguous USA? *International Journal of Climatology,* 29:31–45. doi:10.1002/joc.1696.

R Core Development Team, 2011, R: A Language and Environment for Statistical Computing. http://www.r-project.org/.

Rayner, N.A., Brohan, P., Parker, D., Folland, C.K., Kennedy, J.J., Vanicek, M., Ansell, T.J., and Tett, S., 2005, Improved analyses of changes and uncertainties in sea surface temperature measured in situ since the mid-nineteenth century: The HadSST2 Dataset. *J Climate,* 19:446–469.

Ribatet, M., Sauquet, E., Grésillon, J.-M., and Ouarda, T., 2007, A regional Bayesian POT model for flood frequency analysis. *Stochastic Environmental Research and Risk Assessment,* 21:327–339. doi:10.1007/s00477-006-0068-z.

Robson, A.J., 1999, *Statistical procedures for flood frequency estimation,* Institute of Hydrology, Wallingford, Oxfordshire, OX10 8BB, UK.

Rodda, H.J.E., Little, M.A., Wood, R.G., MacDougall, N., and McSharry, P.E., 2009, A digital archive of extreme rainfalls in the British Isles from 1866 to 1968 based on British Rainfall. *Weather,* 64:71–75. doi:10.1002/wea.354.

Rodriguez-Fonseca, B., and De Castro, M., 2002, On the connection between winter anomalous precipitation in the Iberian Peninsula and North West Africa and the summer subtropical Atlantic sea surface temperature. *Geophys Res Lett,* 29:1863. doi:10.1029/2001gl014421.

Sakalauskiene, G., 2003, The Hurst Phenomenon in Hydrology. *Environmental research, engineering and management,* 25:16–20.

Sapiano, M.R.P., Stephenson, D.B., Grubb, H.J., and Arkin, P.A., 2006, Diagnosis of Variability and Trends in a Global Precipitation Dataset Using a Physically Motivated Statistical Model. *Journal of Climate,* 19:4154–4166. doi:10.1175/JCLI3849.1.

Serinaldi, F. & Kilsby, C.G., 2012, A modular class of multisite monthly rainfall generators for water resource management and impact studies. *Journal of Hydrology*, 464–465, pp.528–540. doi: 10.1016/j.jhydrol.2012.07.043

Serinaldi, F., and Kilsby, C.G., 2013, On the sampling distribution of Allan factor estimator for a homogeneous Poisson process and its use to test inhomogeneities at multiple scales. *Physica A: Statistical Mechanics and its Applications,* 392:1080–1089. doi:10.1016/j.physa.2012.11.015.

Stephenson, D.B., Pavan, V., Collins, M., Junge, M. M., Quadrelli, R., 2006, North Atlantic Oscillation response to transient greenhouse gas forcing and the impact on European winter climate: a CMIP2 multi-model assessment. *Climate Dynamics*, 27(4), pp.401–420.

Tebaldi, C., Hayhoe, K., Arblaster, J., and Meehl, G., 2006, Going to the Extremes. *Climatic Change,* 79:185–211. doi:10.1007/s10584-006-9051-4.

Tramblay, Y., Neppel, L., and Carreau, J., 2011, Brief communication "Climatic covariates for the frequency analysis of heavy rainfall in the Mediterranean region". *Nat Hazards Earth Syst Sci,* 11:2463–2468. doi:10.5194/nhess-11-2463-2011.

Trenberth, K.E., 2011, Attribution of climate variations and trends to human influences and natural variability. *Wiley Interdisciplinary Reviews: Climate Change,* 2:925–930. doi:10.1002/wcc.142.

Underwood, F.M., 2009, Describing long-term trends in precipitation using generalized additive models. *Journal of Hydrology,* 364:285–297. doi:10.1016/j.jhydrol.2008.11.003.

Villarini, G., and Serinaldi, F., 2011, Development of statistical models for at-site probabilistic seasonal rainfall forecast. *International Journal of Climatology,* 32:2197–2212. doi:10.1002/joc.3393.

Villarini, G., Serinaldi, F., Smith, J.A., and Krajewski, W.F., 2009, On the stationarity of annual flood peaks in the continental United States during the 20th century. *Water Resour Res,* 45:W08417. doi:10.1029/2008wr007645.

Villarini, G., Smith, J.A., Vitolo, R., and Stephenson, D.B., 2012, On the temporal clustering of US floods and its relationship to climate teleconnection patterns. *International Journal of Climatology*. doi:10.1002/joc.3458.

Wang, C., and Dong, S., 2010, Is the basin-wide warming in the North Atlantic Ocean related to atmospheric carbon dioxide and global warming? *Geophys Res Lett,* 37. doi:10.1029/2010GL042743.

Wilby, R.L., Conway, D., and Jones, P.D., 2002, Prospects for downscaling seasonal precipitation variability using conditioned weather generator parameters. *Hydrological Processes,* 16:1215–1234. doi:10.1002/hyp.1058.

Wilby, R.L., Wedgbrow, C.S., and Fox, H.R., 2004, Seasonal predictability of the summer hydrometeorology of the River Thames, UK. *Journal of Hydrology,* 295:1–16. doi:10.1016/j.jhydrol.2004.02.015.

Wood, S.N., 2000, Modelling and smoothing parameter estimation with multiple quadratic penalties. *Journal of the Royal Statistical Society: Series B (Statistical Methodology),* 62:413.

Wood, S.N., 2006, Generalized additive models: an introduction with R. Chapman & Hall/CRC.

Wood, S.N., and Augustin, N.H., 2002, GAMs with integrated model selection using penalized regression splines and applications to environmental modelling. *Ecological Modelling,* 157:157–177. doi:10.1016/s0304-3800(02)00193-x.

Yee, T.W., 2010, VGLMs and VGAMs: An overview for applications in fisheries research. *Fisheries Research,* 101:116–126. doi:10.1016/j.fishres.2009.09.015.

Yee, T., 2011, VGAM: Vector Generalized Linear and Additive Models (RDC Team, Ed.). http://cran.r-project.org/package=VGAM.

Yee, T., and Stephenson, A., 2007, Vector generalized linear and additive extreme value models. *Extremes,* 10:1–19. doi:10.1007/s10687-007-0032-4.

Yee, T., and Wild, C.J., 1996, Vector Generalized Additive Models. *J R Statist Soc B,* 58:481–493.

Zhou, L., Dai, A., Dai, Y., Vose, R., Zou, C.-Z., Tian, Y., and Chen, H., 2009, Spatial dependence of diurnal temperature range trends on precipitation from 1950 to 2004. *Climate Dynamics,* 32:429–440. doi:10.1007/s00382-008-0387-5.